Human spermatozoa migration in microchannels reveals boundary-following navigation

Petr Denissenko[a,b,1], Vasily Kantsler[c], David J. Smith[a,b,d], and Jackson Kirkman-Brown[b,e]

[a]School of Engineering, University of Warwick, Coventry CV4 7AL, United Kingdom; [b]Centre for Human Reproductive Science, Birmingham Women's National Health Service Foundation Trust, Mindelsohn Way, Birmingham B15 2TG, United Kingdom; [c]Department of Applied Mathematics and Theoretical Physics, University of Cambridge, Cambridge CB3 0WA, United Kingdom; [d]School of Mathematics, University of Birmingham, Edgbaston, Birmingham B15 2TT, United Kingdom; and [e]School of Clinical and Experimental Medicine, University of Birmingham, Edgbaston, Birmingham, B15 2TT United Kingdom

Edited by David A. Weitz, Harvard University, Cambridge, MA, and approved April 3, 2012 (received for review February 22, 2012)

The migratory abilities of motile human spermatozoa in vivo are essential for natural fertility, but it remains a mystery what properties distinguish the tens of cells which find an egg from the millions of cells ejaculated. To reach the site of fertilization, sperm must traverse narrow and convoluted channels, filled with viscous fluids. To elucidate individual and group behaviors that may occur in the complex three-dimensional female tract environment, we examine the behavior of migrating sperm in assorted microchannel geometries. Cells rarely swim in the central part of the channel cross-section, instead traveling along the intersection of the channel walls ("channel corners"). When the channel turns sharply, cells leave the corner, continuing ahead until hitting the opposite wall of the channel, with a distribution of departure angles, the latter being modulated by fluid viscosity. If the channel bend is smooth, cells depart from the inner wall when the curvature radius is less than a threshold value close to 150 μm. Specific wall shapes are able to preferentially direct motile cells. As a consequence of swimming along the corners, the domain occupied by cells becomes essentially one-dimensional, leading to frequent collisions, and needs to be accounted for when modeling the behavior of populations of migratory cells and considering how sperm populate and navigate the female tract. The combined effect of viscosity and three-dimensional architecture should be accounted for in future in vitro studies of sperm chemoattraction.

cell swimming | motility | reproduction | thigmotaxis

Sperm motility is influenced by surfaces; this is most simply and strikingly evident in the accumulation of cells on the surfaces of microscope slides and coverslips, a phenomenon known to every andrologist. The effect and its causes have been investigated extensively through a variety of approaches, including microscopy (1–4), computational fluid mechanics, (5–9), molecular dynamics (10), and mathematical analysis (11). Principal points addressed by previous studies are the extent to which surface accumulation is a generic feature fluid dynamic effect associated with near-wall swimming, the role of specialized flagellar beat patterns, species-specific morphology, and the relative prevalence of swimming "near" as opposed to "against" walls; discussion of these questions can be found in recent editorials (12, 13). There has also been a resurgence of interest recently in the fluid mechanics of motile bacteria (14–17) and generic models for swimming cells (11, 18–20).

Previous studies have usually focused on the behavior of a cell near a single planar surface or between a pair of planar surfaces, modeling the interior of a haemocytometer or similar device; however, both the female reproductive tract and microfluidic in vitro fertilization (IVF) devices present sperm with a much more confined and potentially tortuous geometry. The fallopian tubes consist of ciliated epithelium (21), the distance between opposed epithelial surfaces being of the order of 100 μm in many regions, particularly cervical crypts and the folds of the ampullary fallopian tube, comparable with the approximate 50-μm length of the human sperm flagellum. Microchannel fabrication technology also allows the construction of environments with complex geometries that may be exploited in directing and sorting cells (22). In this paper, we report experimental observations of the motility of populations of human sperm in fabricated microchannel environments and the effect of fluid viscosity.

Bacterial cell movement in microchannels, particularly those produced with soft lithography, has perhaps received more attention than sperm, and studies have focused more closely on cell tracking and motility characteristics in the channels. Galajda et al. (23) showed that a "wall of funnels" can be used to concentrate bacteria preferentially on one side, producing a nonuniform distribution from an initially uniform one—an apparent example of "Maxwell's Demon." Hulme et al. (22) showed that a "ratchet" geometry microchannel can be used to direct bacterial movement, and that cells can be sorted by length through their ability to navigate different curvature bends, purely on the basis of cell motility and surface interaction; no external pumping was required. Recently, Binz et al. (24) investigated the effect of channel width and path tortuosity on *Serratia marcescens* migration in polydimethylsiloxane (PDMS) microenvironments. These studies lead us to ask the following questions: What principles govern sperm motility in microchannel environments, how might they be exploited in IVF technology, and how might they extrapolate to understanding the migration of sperm to the egg?

Results

The first observation is that cells mainly swim along the channel corners as sketched in Fig. 1*A*. Indeed, contours of the channel appear black (Fig. 2*A*), which indicates that many cells passed during the imaging period, as red, green, and blue stains combine to give black. At the periphery of the frame, due to the short distance between objective and the channel, the vertical channel wall is visible, enabling us to distinguish cells swimming in the "top" and "bottom" corners of the channel: We see two parallel bunches of cell tracks indicated in Fig. 2*B*. Swimming can be characterized as being almost *against* rather than simply *near* walls, similar to chinchilla sperm observations of Woolley (4), and differing from the mixture of near- and against-wall swimming evident from experiment (2) in 400-μm capillary tubes and computation (7). This disparity may be due to the presence of vertical in addition to horizontal walls, and emphasizes the difference between motility in standard (broad) in vitro environments, where vertical walls are usually not an immediate influencing factor, and hence the cells traverse a 2D wall, as opposed to con-

Author contributions: P.D. designed research; P.D. performed research; V.K., D.J.S., and J.K.-B. contributed new reagents/analytic tools; P.D., V.K., D.J.S., and J.K.-B. analyzed data; and P.D., D.J.S., and J.K.-B. wrote the paper.

The authors declare no conflict of interest.

This article is a PNAS Direct Submission.

[1]To whom correspondence should be addressed. E-mail: p.denissenko@warwick.ac.uk.

This article contains supporting information online at www.pnas.org/lookup/suppl/doi:10.1073/pnas.1202934109/-/DCSupplemental.

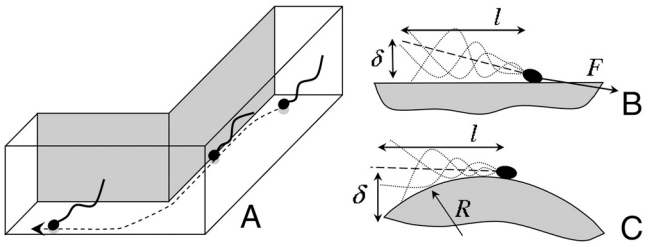

Fig. 1. Schematic of inferred cell migratory behavior. Cells swim head against the wall, ending up swimming along corners; on sharp turns, cells depart from channel walls (*A*). Qualitative explanation of why the cells swim head against the wall (*B*) and an estimate of the cell minimum turning radius (*C*).

fined spaces of artificial microchannels and female tract physiology where the cell will experience a complex 3D series of surfaces.

The next clearly observed effect is that cells depart from walls on sharp turns forming "fans" of trajectories, indicated in Fig. 2*C*. After reaching the opposite wall, most cells follow it to the next turn. As a result, few or no cells swim along "inner" segments of channel walls (Fig. 2*D*). On curved turns, cells may also depart the channel wall (Fig. 2*E*) though some cells still continue following the wall. Sometimes cells leave the corner in the absence of geometrical features (Fig. 2*F*), which we attribute to collisions. These collisions may be head-on or overtaking, as shown in Fig. 3.

The fact that cells depart from corners can be used to create a channel with ratchet-type walls to force cells to swim in one direction. Cells in a sort of a circular running track are shown in Fig. 4. Certain configurations lead to entrapment of cells for extended times. A defective link in an earlier version of a channel was able to trap cells for as long as 10 min before they escaped: Two crypts on the opposite walls were staggered in such a way that, while following the channel wall, a cell was ejected by one crypt to get into the other and then ejected by the latter to return to the first crypt.

We have studied the influence of medium rheology on the cell near-wall behavior by filling the microchannel with 0%, 0.5%, and 1.0% solutions of methylcellulose. The main effects are shown to be robust with respect to medium rheology: Spermatozoa swim head-against-the-wall and depart from sharp bends in both pure (Newtonian) medium and in the medium with methyl-

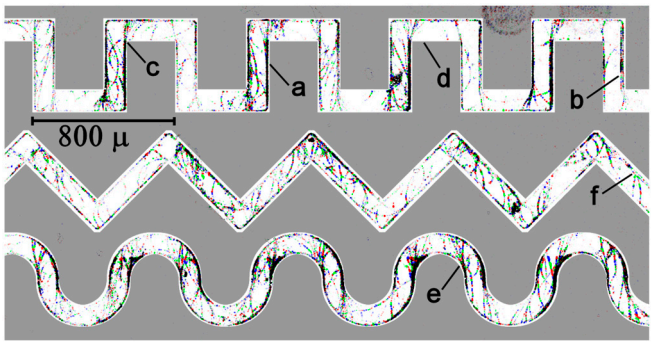

Fig. 2. A typical superposition of an image sequence; top view of the microchannel. Cell positions in successive frames are color-coded as red-green-blue to resolve the swimming direction. The space between microchannels is shaded gray to indicate position of walls. Edges of gray shading are spaced from channel walls by approximately 15 μm so that they do not interfere with tracks of the cells. Most of cells swim along the intersection of the channel vertical and horizontal walls (*A*) with few tracks observed in the middle of the channel. At the periphery of the image where the "side" wall of the channel is observed at an angle, cells traveling along in top and bottom corners between channel walls can be distinguished (*B*). When the channel turns, cells depart from the wall (*C*). As a result, no cells travel along the inner corners after the turn (*D*). In a curved channel, some cells continue to travel along the wall and some depart (*E*). Cells may also depart from the wall on collision with each other (*F*) which is shown in Fig. 3 with a greater magnification.

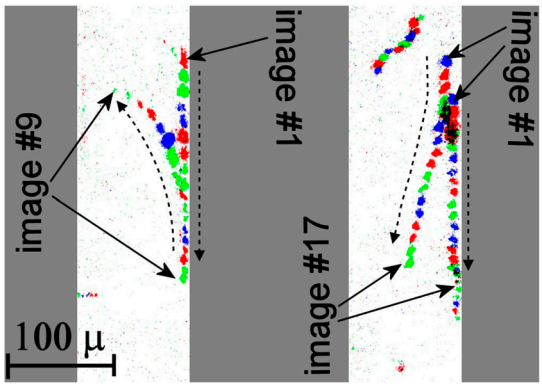

Fig. 3. Cells may depart from walls on collision. The image on the left is composed of nine consequent frames and shows a head-on collision; here, the beginning of the track of the departed cell is overdrawn by the track of the cell that stayed attached and is not visible. The image on the right is composed of 17 consequent frames and shows a collision when one sperm cell overtakes another. The time interval between images is one-quarter of a second. Cell swimming directions are indicated with dotted arrows; positions of the cells in first and last images of sequences are indicated by solid arrows. Location of the channel walls are indicated by gray shading.

cellulose, which has more than 100 times higher viscosity and complicated rheological properties. A qualitative observation is that, at higher concentration of methylcellulose, visibly more cells swim in the middle of the channel. To assess the distribution of cells departing from walls on the channel bends, we analyze the pixel intensity in fans of trajectories starting from channel bends in superposition of image sequences. Because the light sensitivity of our CCD camera is linear to a good approximation, pixel intensity is a suitable quantitative parameter to use for reconstruction of the cell distribution by departure angles. The 30-min-long records have been analyzed and data over four 90° channel bends have been analyzed. Typical results are shown in Fig. 5. Depending on the donor, the mean cell turning angle varies from 10° to 20° with the width at half maximum at the level of 25°. Observe

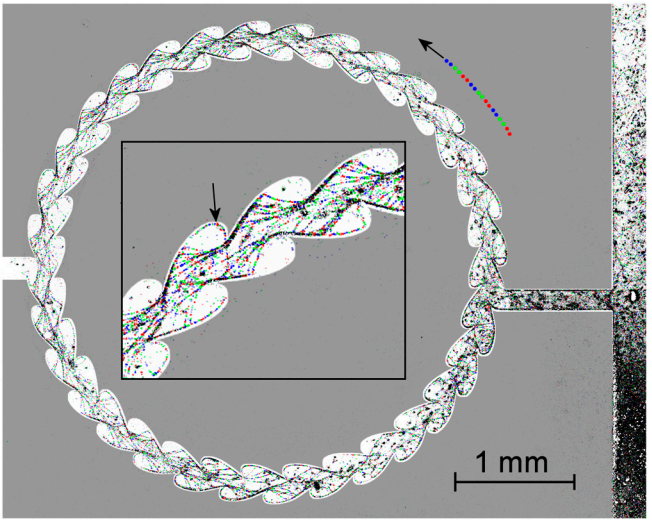

Fig. 4. Spermatozoa in the "one way running track" microchannel geometry. The space outside the microchannel is shaded gray to indicate position of the walls. Edges of gray shading are spaced from channel walls by approximately 10–20 μm so that they do not interfere with tracks of the cells. The long arrow shows the preferred (counterclockwise) direction of cell migration. The arrow in the zoomed insert of the channel segment points at a track of a cell swimming in the direction opposite to that dictated by features of channel walls. Follow the track to see this cell departing from the inside of the ratchet and traversing the channel, being redirected counterclockwise, as the other cells travel.

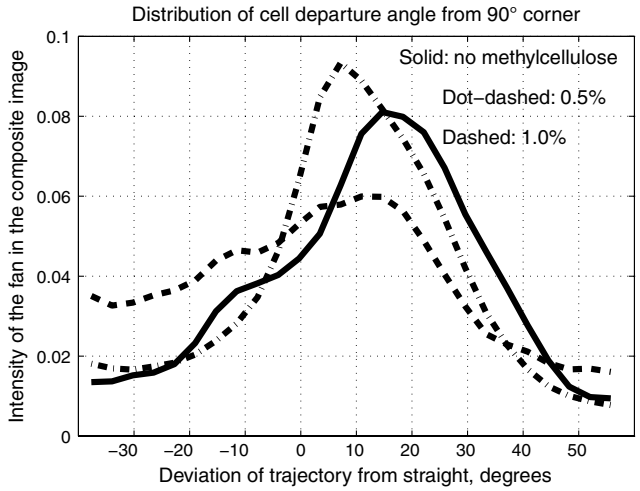

Fig. 5. Distribution of the angle of cell departure from the inner wall on a 90° bend of the channel. Zero angle corresponds to the cell continuing motion without turning; positive angles correspond to cells turning in the same direction as the channel bends.

that a notable part of cells turn away from the wall (negative angles). Although addition of methylcellulose definitely affects the distribution, no consistent dependence of departure angles on the concentration has been detected; methylcellulose affected spermatozoa from different donors in different ways. This variability may be attributed to a sophisticated interplay of the medium rheological properties with the head shape and flagellum stroke pattern that are individual for different donors.

Discussion

We can interpret our observations through the following intuitive model, similar to that advanced by Woolley (4). The amplitude of head oscillations is less than that of the end of the tail, so the head can, on average, be closer to the wall. The conical envelope of the flagellar wave aligns with the surface, resulting in the direction of propulsion being inclined toward the wall (Fig. 1*B*). Cells therefore are directed toward surfaces and, moreover, cells stay against those surfaces. Once a cell reaches a horizontal wall, it is likely to travel along horizontally while translating until it, by chance, reaches a vertical wall (or vice versa). It then remains trapped by both walls, swimming along their intersection, until it finally reaches a sufficiently sharp change to the curvature of a vertical wall (Fig. 1*A*) to cause departure.

Furthermore, we can use this intuitive model to estimate the minimum turning radius of the cell. Consider similar triangles, the one formed by the cell envelope and the one formed by radii connecting head and tail of the cell with the center of a circle forming the channel wall (Fig. 1*C*). Equating the ratios of triangle bases and sides, we get that the radius of the channel wall R at which a cell of the length ℓ is oriented tangent to the surface at the point of the head contact can be estimated as

$$\frac{\delta}{\ell} \approx \frac{\ell/2}{R} \Rightarrow R \approx \frac{\ell}{2\delta}\ell. \qquad [1]$$

Substituting $\ell = 50$ μm and $\ell/2\delta \sim 3$ from microscopic observations, we get $R \sim 150$ μm. This value is close to the inner radius of curved (the lowest) channel in Fig. 2. Observe that, although most cells depart on the turn, some stay at the wall, which is an indication that the wall radius is not far from critical in accordance with the estimate [**1**].

The effect of viscosity on cell departure angle emphasizes the need to perform laboratory assays and ex vivo sperm-tract interaction studies in medium with rheology adjusted to that of physiological fluids. Indeed, the shear rate in the fluid surrounding spermatozoa changes from 1,000 s^{-1} in the vicinity of flagellum to 10 s^{-1} in the vicinity of the head and some intermediate value in the gap between the head and the channel wall, so that viscosity of 1% methylcellulose changes fourfold from 0.12 to 0.5 Pa·s (25). As a result, a particular shape of sperm head and a particular waveform of flagellum beat would affect the dynamics of cell motion when following walls and departing from walls in a sophisticated way, so that departure angles depend not only on fluid properties, but also on fine features of spermatozoa constitution subject to within- and between-donor heterogeneity. This dependence can be exploited as a basis for diagnostic criteria; for example, head shape depends on the quality of DNA packing. Mathematical models of sperm motility in rheologically complex fluids are in development in our group.

Variation in departure angles also suggests a possible role for medium rheology in deflecting cells away from crypts in the reproductive tract. Our finding that sperm respond to ratchet geometries in a similar way to bacteria may potentially improve microfluidic IVF devices, through acting to direct high concentrations of motile cells toward the egg.

Medium containing 1% methylcellulose has been shown by both a migration study (26) and oscillatory rheometry (27) to be a useful mimic of cervical mucus. Although we are not aware of data on the rheological properties of oviductal fluid, it is likely to vary significantly during the menstrual cycle, evidenced by observations of estrogen-dependent cyclic secretion of luminal mucus in the human isthmus (28); these changes may have functional relevance for sperm migration.

Incubation-induced capacitation, and the associated motility change of hyperactivation, have been associated with an increased proportion of cells to penetrate highly viscous and viscoelastic fluids (29), with capacitation manifesting as rapid progressive motility in sufficiently viscous fluid. Capacitating conditions were not used in our experiments, which interfaced semen and medium directly, moreover rates of hyperactivation in human sperm incubated in this way are generally only of the order of 5%. Capacitation may therefore not be required for migration through viscous medium, however, it may result in altered motility characteristics and resulting migratory behavior, being of potential special significance in the fallopian tubes and cumulus penetration; a full investigation is beyond the scope of the present study.

We only have the beginnings of an understanding of how the minute population of sperm reaching the site of fertilization may differ from the vast majority that do not. The existence of this distinguished subpopulation was suggested by in vivo studies in rabbits (30) over 30 y ago, but the determinants of successful migration still remain mysterious; these characteristics may include motility, in addition to immunological markers and morphology. Further experimentation may also enable development of a useful motility-based functional diagnostic or prognostic test for male fecundity. For example, observation of sperm in microchannels may reveal hitherto undiscovered swimming parameters underlying successful tract migration or navigation.

As shown above, sperm cell migration in a microchannel crucially depends on the channel geometry. Cells swim along boundaries and, if the two flat boundaries intersect, cells follow the corner; this has cardinal consequences for modeling of the cell behavior. Instead of spreading through a three-dimensional domain, many cells swim along one-dimensional folds. First, this boundary-following tendency entails that wall features such as ratchets can prescribe swimming direction. Second, the size of the domain available to the swimmers is drastically reduced, so cells collide more often; this requires special consideration when modeling the spreading of the entire population, either in microchannel environments or the female reproductive tract. The increased likelihood of a sperm–sperm collision may also have a more complex behavioral effect; when cells collide, mechano-

transduction may induce cell signaling, altering beat pattern and hence migratory behavior.

The findings now indicate that recent advances in investigating sperm chemoattractants not only need to take account of the rheology of the fluid in which the cells are swimming (31), but also the three-dimensional architecture of the fluid domain. The application of experimental and computational fluid dynamics is beginning to reveal the complexity of the system of sperm-tract interaction, one of the central unsolved problems in reproductive science.

Materials and Methods

This study employed channels of a cross-section 100 × 100 μm to observe trajectories of individual freely migrating human sperm in microchannels of basic geometrical configurations (corners, curves) and more complex features (ratchets). Cell behavior in microchannels of basic geometrical configurations was studied. Microchannels of 100-μm height were produced in elastomer (PDMS) by soft lithography (32) and then bonded to a glass coverslip after oxygen plasma treatment. Swimming cells were observed through the glass wall of the channel using a CCD camera equipped with a standard microscope objective. A green 100-mW diode laser equipped with a condenser was used as the light source. For imaging of the whole channel, we utilized a 160 mm 2× objective attached with an extension tube to a four Megapixel Basler avA2300-25gm camera run at four frames per second. Cell swimming was examined in fluid of three different rheologies: 0%, 0.5%, and 1% methylcellulose (M0512; Sigma-Aldrich; approximate molecular weight 88,000) was added to Earle's Balanced Salt Solution without phenol red, supplemented with 2.5 mM Na pyruvate and 19 mM Na lactate (06-2010-03-1B; Biological Industries), and 0.3% wt/vol charcoal delipidated bovine serum albumin (Sigma; A7906). Semen samples were obtained by masturbation, at the Centre for Human Reproductive Science, Birmingham Women's National Health Service Foundation Trust from normozoospermic research donors giving informed consent, after 2- to 4-d abstinence. Donors provided informed consent under Local Ethical Approval (South Birmingham Local Research Ethics Committee 2003/239). Experiments were performed between 1 and 3 h after the semen sample was produced. The raw semen was injected into the wide "entry" branch of the channel from which cells naturally spread to the main section. Results shown are representative of five donors.

Acquired images were processed in series of 200 to form superimposition images. Pixels at which the brightness increased from frame n to frame $n + 1$ above a certain level were stained, so that only moving objects are visible. Additionally, the image sequence was color coded as follows: Cell positions in frames 1 and 2 are stained red, frames 3 and 4 green, frames 5 and 6 blue, frames 7 and 8 red again, and so on. Hence, the direction of cell motion can be inferred from superposition images. One such image is shown in Fig. 2. Camera resolution was 2.7 μm per pixel, too coarse to resolve details of the cell head, but sufficient to determine its position.

ACKNOWLEDGMENTS. The authors thank staff at Birmingham Women's Hospital and members of the Centre for Human Reproductive Science, University of Birmingham, for assistance; the authors also thank Prof. Howard Berg for comments on the manuscript. J.K.-B. acknowledges funding from Birmingham Science City Translational Medicine Clinical Research Infrastructure and Trials Platform, with support from Advantage West Midlands; D.J.S. acknowledges a Birmingham Science City Fellowship; P.D. acknowledges funding from Warwick Institute of Advanced Study.

1. Rothschild L (1963) Non-random distribution of bull spermatozoa in a drop of sperm suspension. *Nature* 198:1221–1222.
2. Winet H, Bernstein GS, Head J (1984) Observations on the response of human spermatozoa to gravity, boundaries and fluid shear. *J Reprod Fertil* 70:511–523.
3. Cosson J, Huitorel P, Gagnon C (2003) How spermatozoa come to be confined to surfaces. *Cell Motil Cytoskeleton* 54:56–63.
4. Woolley DM (2003) Motility of spermatozoa at surfaces. *Reproduction* 126:259–270.
5. Ramia M, Tullock DL, Phan-Thien N (1993) The role of hydrodynamic interaction in the locomotion of microorganisms. *Biophys J* 65:755–778.
6. Fauci LJ, McDonald A (1995) Sperm motility in the presence of boundaries. *Bull Math Biol* 57:679–699.
7. Smith DJ, Gaffney EA, Blake JR, Kirkman-Brown JC (2009) Human sperm accumulation near surfaces: A simulation study. *J Fluid Mech* 621:220–236.
8. Smith DJ, Blake JR (2009) Surface accumulation of spermatozoa: A fluid dynamic phenomenon. *Math Sci* 465:2417–2439.
9. Blake JR (1971) A note on the image system for a Stokeslet in a no-slip boundary. *Proc Cambridge Philos Soc* 70:303–310.
10. Elgeti J, . Kaupp UB, Gompper G (2010) Hydrodynamics of sperm cells near surfaces. *Biophys J* 99:1018–1026.
11. Crowdy DG, Or Y (2010) Two-dimensional point singularity model of a low-Reynolds-number swimmer near a wall. *Phys Rev E Stat Nonlin Soft Matter Phys* 81:036313.
12. Smith DJ, Gaffney EA, Shum H, Gadêlha H, Kirkman-Brown J (2011) Comment on the article by J. Elgeti et al. Hydrodynamics of sperm cells near surfaces. *Biophys J* 100:2318–2320.
13. Elgeti J, Kaupp UB, Gompper G (2011) Response to comment on article: Hydrodynamics of sperm cells near surfaces. *Biophys J* 100:2321–2324.
14. Lauga E, DiLuzio WR, Whitesides GM, Stone HA (2006) Swimming in circles: Motion of bacteria near solid boundaries. *Biophys J* 90:400–412.
15. Guanglai Li, Tang Jay X (2009) Accumulation of microswimmers near a surface mediated by collision and rotational brownian motion. *Phys Rev Lett* 103:078101.
16. Giacché D, Ishikawa T, Yamaguchi T (2010) Hydrodynamic entrapment of bacteria swimming near a solid surface. *Phys Rev E Stat Nonlin Soft Matter Phys* 82:56309.
17. Shum H, Gaffney EA, Smith DJ (2010) Modelling bacterial behaviour close to a no-slip plane boundary: The influence of bacterial geometry. *Proc R Soc London Ser A* 466:1725–1748.
18. Berke AP, Turner L, Berg HC, Lauga E (2008) Hydrodynamic attraction of swimming microorganisms by surfaces. *Phys Rev Lett* 101:38102.
19. Or Y, Murray RM (2009) Dynamics and stability of a class of low Reynolds number swimmers near a wall. *Phys Rev E Stat Nonlin Soft Matter Phys* 79:045302(R).
20. Crowdy D, Samson O (2011) Hydrodynamic bound states of a low-reynolds-number swimmer near a gap in a wall. *J Fluid Mech* 667:309–335.
21. Suarez SS, Pacey AA (2006) Sperm transport in the female reproductive tract. *Hum Reprod Update* 12:23–37.
22. Hulme SE, et al. (2008) Using ratchets and sorters to fractionate motile cells of escherichia coli by length. *Lab Chip* 8:1888–1895.
23. Galajda P, Keymer J, Chaikin P, Austin R (2007) A wall of funnels concentrates swimming bacteria. *J Bacteriol* 189:8704–8707.
24. Binz M, Lee AP, Edwards C, Nicolau DV (2010) Motility of bacteria in microfluidic structures. *Microelectron Eng* 87:8810–8813.
25. Renliang L, Tu L, Fengyuan Y, Hongbin Z (2011) Rheological and microdsc studies on the aqueous mixtures of methylcellulose and ammonium poly(3-thiophene acetic acid). *Carbohydr Polym* 85:862–868.
26. Ivic A, et al. (2002) Critical evaluation of methylcellulose as an alternative medium in sperm migration tests. *Hum Reprod* 17:143–149.
27. Smith DJ, Gaffney EA, Gadêlha H, Kapur N, Kirkman-Brown JC (2009) Bend propagation in the flagella of migrating human sperm, and its modulation by viscosity. *Cell Motil Cytoskeleton* 66:220–236.
28. Jansen RPS (1980) Cyclic changes in the human fallopian tube isthmus and their functional importance. *Am J Obstet Gynecol* 136:292–308.
29. Suarez SS, Dai X (1992) Hyperactivation enhances mouse sperm capacity for penetrating viscoelastic media. *Biol Reprod* 46:686–691.
30. Cohen J, Tyler KR (1980) Sperm populations in the female genital tract of the rabbit. *J Reprod Fertil* 60:213–218.
31. Kirkman-Brown JC, Smith DJ (2011) Sperm motility: Is viscosity fundamental to progress? *Mol Hum Reprod* 17:539–544.
32. Xia YN, Whitesides GM (1998) Soft lithography. *Annu Rev Mater Sci* 28:153–184.